1998; Weickert 1998). It has also been shown to be closely related to other *adaptive smoothing* techniques (Saint-Marc, Chen, and Medioni 1991; Barash 2002; Barash and Comaniciu 2004) as well as Bayesian regularization with a non-linear smoothness term that can be derived from image statistics (Scharr, Black, and Haussecker 2003).

In its general form, the range kernel $r(i, j, k, l) = r(\|f(i, j) - f(k, l)\|)$, which is usually called the *gain* or *edge-stopping* function, or diffusion coefficient, can be any monotonically increasing function with $r'(x) \to 0$ as $x \to \infty$. Black, Sapiro, Marimont *et al.* (1998) show how anisotropic diffusion is equivalent to minimizing a robust penalty function on the image gradients, which we discuss in Sections 3.7.1 and 3.7.2). Scharr, Black, and Haussecker (2003) show how the edge-stopping function can be derived in a principled manner from local image statistics. They also extend the diffusion neighborhood from $\mathcal{N}_4$ to $\mathcal{N}_8$, which allows them to create a diffusion operator that is both rotationally invariant and incorporates information about the eigenvalues of the local structure tensor.

Note that, without a bias term towards the original image, anisotropic diffusion and iterative adaptive smoothing converge to a constant image. Unless a small number of iterations is used (e.g., for speed), it is usually preferable to formulate the smoothing problem as a joint minimization of a smoothness term and a data fidelity term, as discussed in Sections 3.7.1 and 3.7.2 and by Scharr, Black, and Haussecker (2003), which introduce such a bias in a principled manner.

3.3.2 Morphology

While non-linear filters are often used to enhance grayscale and color images, they are also used extensively to process binary images. Such images often occur after a *thresholding* operation,

$$\theta(f, t) = \begin{cases} 1 & \text{if } f \geq t, \\ 0 & \text{else,} \end{cases} \tag{3.41}$$

e.g., converting a scanned grayscale document into a binary image for further processing such as *optical character recognition*.

The most common binary image operations are called *morphological operations*, since they change the *shape* of the underlying binary objects (Ritter and Wilson 2000, Chapter 7). To perform such an operation, we first convolve the binary image with a binary *structuring element* and then select a binary output value depending on the thresholded result of the convolution. (This is not the usual way in which these operations are described, but I find it a nice simple way to unify the processes.) The structuring element can be any shape, from a simple 3×3 box filter, to more complicated disc structures. It can even correspond to a particular shape that is being sought for in the image.

Figure 3.21 shows a close-up of the convolution of a binary image f with a 3×3 structuring element s and the resulting images for the operations described below. Let

$$c = f \otimes s \tag{3.42}$$

be the integer-valued *count* of the number of 1s inside each structuring element as it is scanned over the image and S be the size of the structuring element (number of pixels). The standard operations used in binary morphology include:

- **dilation**: $\text{dilate}(f, s) = \theta(c, 1)$;

(a) (b) (c) (d) (e) (f)

Figure 3.21 Binary image morphology: (a) original image; (b) dilation; (c) erosion; (d) majority; (e) opening; (f) closing. The structuring element for all examples is a 5×5 square. The effects of majority are a subtle rounding of sharp corners. Opening fails to eliminate the dot, since it is not wide enough.

- **erosion**: $\text{erode}(f, s) = \theta(c, S)$;
- **majority**: $\text{maj}(f, s) = \theta(c, S/2)$;
- **opening**: $\text{open}(f, s) = \text{dilate}(\text{erode}(f, s), s)$;
- **closing**: $\text{close}(f, s) = \text{erode}(\text{dilate}(f, s), s)$.

As we can see from Figure 3.21, dilation grows (thickens) objects consisting of 1s, while erosion shrinks (thins) them. The opening and closing operations tend to leave large regions and smooth boundaries unaffected, while removing small objects or holes and smoothing boundaries.

While we will not use mathematical morphology much in the rest of this book, it is a handy tool to have around whenever you need to clean up some thresholded images. You can find additional details on morphology in other textbooks on computer vision and image processing (Haralick and Shapiro 1992, Section 5.2) (Bovik 2000, Section 2.2) (Ritter and Wilson 2000, Section 7) as well as articles and books specifically on this topic (Serra 1982; Serra and Vincent 1992; Yuille, Vincent, and Geiger 1992; Soille 2006).

3.3.3 Distance transforms

The distance transform is useful in quickly precomputing the distance to a curve or set of points using a two-pass raster algorithm (Rosenfeld and Pfaltz 1966; Danielsson 1980; Borgefors 1986; Paglieroni 1992; Breu, Gil, Kirkpatrick *et al.* 1995; Felzenszwalb and Huttenlocher 2004a; Fabbri, Costa, Torelli *et al.* 2008). It has many applications, including level sets (Section 5.1.4), fast *chamfer matching* (binary image alignment) (Huttenlocher, Klanderman, and Rucklidge 1993), feathering in image stitching and blending (Section 9.3.2), and nearest point alignment (Section 12.2.1).

The distance transform $D(i, j)$ of a binary image $b(i, j)$ is defined as follows. Let $d(k, l)$ be some *distance metric* between pixel offsets. Two commonly used metrics include the *city block* or *Manhattan* distance

$$d_1(k, l) = |k| + |l| \tag{3.43}$$

and the *Euclidean* distance

$$d_2(k, l) = \sqrt{k^2 + l^2}. \tag{3.44}$$

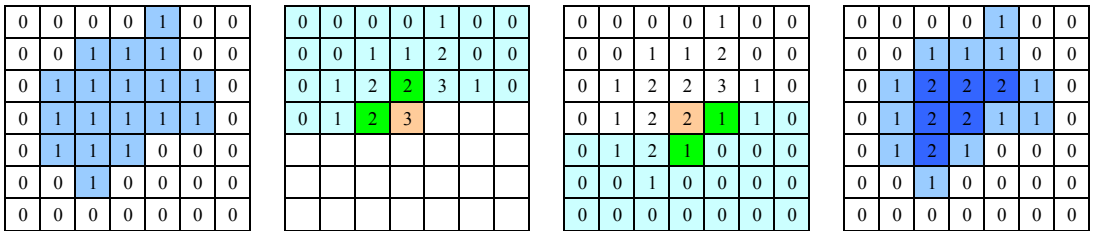

Figure 3.22 City block distance transform: (a) original binary image; (b) top to bottom (forward) raster sweep: green values are used to compute the orange value; (c) bottom to top (backward) raster sweep: green values are merged with old orange value; (d) final distance transform.

The distance transform is then defined as

$$D(i,j) = \min_{k,l:b(k,l)=0} d(i-k, j-l), \tag{3.45}$$

i.e., it is the distance to the *nearest* background pixel whose value is 0.

The D_1 city block distance transform can be efficiently computed using a forward and backward pass of a simple raster-scan algorithm, as shown in Figure 3.22. During the forward pass, each non-zero pixel in b is replaced by the minimum of 1 + the distance of its north or west neighbor. During the backward pass, the same occurs, except that the minimum is both over the current value D and 1 + the distance of the south and east neighbors (Figure 3.22).

Efficiently computing the Euclidean distance transform is more complicated. Here, just keeping the minimum scalar distance to the boundary during the two passes is not sufficient. Instead, a *vector-valued* distance consisting of both the x and y coordinates of the distance to the boundary must be kept and compared using the squared distance (hypotenuse) rule. As well, larger search regions need to be used to obtain reasonable results. Rather than explaining the algorithm (Danielsson 1980; Borgefors 1986) in more detail, we leave it as an exercise for the motivated reader (Exercise 3.13).

Figure 3.11g shows a distance transform computed from a binary image. Notice how the values grow away from the black (ink) regions and form ridges in the white area of the original image. Because of this linear growth from the starting boundary pixels, the distance transform is also sometimes known as the *grassfire transform*, since it describes the time at which a fire starting inside the black region would consume any given pixel, or a *chamfer*, because it resembles similar shapes used in woodworking and industrial design. The ridges in the distance transform become the *skeleton* (or *medial axis transform (MAT)*) of the region where the transform is computed, and consist of pixels that are of equal distance to two (or more) boundaries (Tek and Kimia 2003; Sebastian and Kimia 2005).

A useful extension of the basic distance transform is the *signed distance transform*, which computes distances to boundary pixels for *all* the pixels (Lavallée and Szeliski 1995). The simplest way to create this is to compute the distance transforms for both the original binary image and its complement and to negate one of them before combining. Because such distance fields tend to be smooth, it is possible to store them more compactly (with minimal loss in *relative* accuracy) using a spline defined over a quadtree or octree data structure

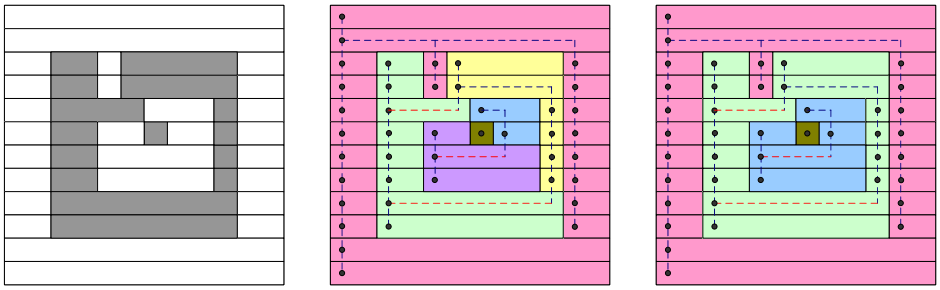

(a) (b) (c)

Figure 3.23 Connected component computation: (a) original grayscale image; (b) horizontal runs (nodes) connected by vertical (graph) edges (dashed blue)—runs are pseudocolored with unique colors inherited from parent nodes; (c) re-coloring after merging adjacent segments.

(Lavallée and Szeliski 1995; Szeliski and Lavallée 1996; Frisken, Perry, Rockwood *et al.* 2000). Such precomputed signed distance transforms can be extremely useful in efficiently aligning and merging 2D curves and 3D surfaces (Huttenlocher, Klanderman, and Rucklidge 1993; Szeliski and Lavallée 1996; Curless and Levoy 1996), especially if the *vectorial* version of the distance transform, i.e., a pointer from each pixel or voxel to the nearest boundary or surface element, is stored and interpolated. Signed distance fields are also an essential component of level set evolution (Section 5.1.4), where they are called *characteristic functions*.

3.3.4 Connected components

Another useful semi-global image operation is finding *connected components*, which are defined as regions of adjacent pixels that have the same input value (or label). (In the remainder of this section, consider pixels to be *adjacent* if they are immediate $\mathcal{N}_4$ neighbors and they have the same input value.) Connected components can be used in a variety of applications, such as finding individual letters in a scanned document or finding objects (say, cells) in a thresholded image and computing their area statistics.

Consider the grayscale image in Figure 3.23a. There are four connected components in this figure: the outermost set of white pixels, the large ring of gray pixels, the white enclosed region, and the single gray pixel. These are shown pseudocolored in Figure 3.23c as pink, green, blue, and brown.

To compute the connected components of an image, we first (conceptually) split the image into horizontal *runs* of adjacent pixels, and then color the runs with unique labels, re-using the labels of vertically adjacent runs whenever possible. In a second phase, adjacent runs of different colors are then merged.

While this description is a little sketchy, it should be enough to enable a motivated student to implement this algorithm (Exercise 3.14). Haralick and Shapiro (1992, Section 2.3) give a much longer description of various connected component algorithms, including ones that avoid the creation of a potentially large re-coloring (equivalence) table. Well-debugged connected component algorithms are also available in most image processing libraries.

Once a binary or multi-valued image has been segmented into its connected components,

it is often useful to compute the area statistics for each individual region $\mathcal{R}$. Such statistics include:

- the area (number of pixels);
- the perimeter (number of boundary pixels);
- the centroid (average x and y values);
- the second moments,

$$\boldsymbol{M} = \sum_{(x,y)\in\mathcal{R}} \begin{bmatrix} x-\overline{x} \\ y-\overline{y} \end{bmatrix} \begin{bmatrix} x-\overline{x} & y-\overline{y} \end{bmatrix}, \tag{3.46}$$

  from which the major and minor axis orientation and lengths can be computed using eigenvalue analysis.[7]

These statistics can then be used for further processing, e.g., for sorting the regions by the area size (to consider the largest regions first) or for preliminary matching of regions in different images.

3.4 Fourier transforms

In Section 3.2, we mentioned that Fourier analysis could be used to analyze the frequency characteristics of various filters. In this section, we explain both how Fourier analysis lets us determine these characteristics (or equivalently, the frequency *content* of an image) and how using the Fast Fourier Transform (FFT) lets us perform large-kernel convolutions in time that is independent of the kernel's size. More comprehensive introductions to Fourier transforms are provided by Bracewell (1986); Glassner (1995); Oppenheim and Schafer (1996); Oppenheim, Schafer, and Buck (1999).

How can we analyze what a given filter does to high, medium, and low frequencies? The answer is to simply pass a sinusoid of known frequency through the filter and to observe by how much it is attenuated. Let

$$s(x) = \sin(2\pi f x + \phi_i) = \sin(\omega x + \phi_i) \tag{3.47}$$

be the input sinusoid whose *frequency* is f, *angular frequency* is $\omega = 2\pi f$, and *phase* is ϕ_i. Note that in this section, we use the variables x and y to denote the spatial coordinates of an image, rather than i and j as in the previous sections. This is both because the letters i and j are used for the *imaginary* number (the usage depends on whether you are reading complex variables or electrical engineering literature) and because it is clearer how to distinguish the horizontal (x) and vertical (y) components in frequency space. In this section, we use the letter j for the imaginary number, since that is the form more commonly found in the signal processing literature (Bracewell 1986; Oppenheim and Schafer 1996; Oppenheim, Schafer, and Buck 1999).

[7] Moments can also be computed using Green's theorem applied to the boundary pixels (Yang and Albregtsen 1996).